Microstructural Development: Organizational Differences of the Fiber Architecture Between Children and Adults in Dorsal and Ventral Visual Streams

Thomas Loenneker,[1,2] **Peter Klaver,**[1,2,3*] **Kerstin Bucher,**[1] **Janine Lichtensteiger,**[1] **Adrian Imfeld,**[3] **and Ernst Martin**[1,2]

[1]*MR Centre, University Children's Hospital Zurich, Zurich, Switzerland*
[2]*Center for Integrative Human Physiology, University of Zurich, Zurich, Switzerland*
[3]*Institute of Psychology, University of Zurich, Zurich, Switzerland*

Abstract: Visual perceptual skills are basically mature by the age of 7 years. White matter, however, continues to develop until late adolescence. Here, we examined children (aged 5–7 years) and adults (aged 20–30 years) using diffusion tensor imaging (DTI) fiber tracking to investigate the microstructural maturation of the visual system. We characterized the brain volumes, DTI indices, and architecture of visual fiber tracts passing through white matter structures adjacent to occipital and parietal cortex (dorsal stream), and to occipital and temporal cortex (ventral stream). Dorsal, but not ventral visual stream pathways were found to increase in volume during maturation. DTI indices revealed expected maturational differences, manifested as decreased mean and radial diffusivities and increased fractional anisotropy in both streams. Additionally, fractional anisotropy was increased and radial diffusivity was decreased in the adult dorsal stream, which can be explained by specific dorsal stream myelination or increasing fiber compaction. Adult dorsal stream architecture showed additional intra- and interhemispheric connections: Dorsal fibers penetrated into contralateral hemispheres via commissural structures and projection fibers extended to the superior temporal gyrus and ventral association pathways. Moreover, intra-hemispheric connectivity was particularly strong in adult dorsal stream of the right hemisphere. Ventral stream architecture also differed between adults and children. Adults revealed additional connections to posterior lateral areas (occipital-temporal gyrus), whereas children showed connections to posterior medial areas (posterior parahippocampal and lingual gyrus). Hence, in addition to dorsal stream myelination or fiber compaction, progressing maturation of intra- and interhemispheric connectivity may contribute to the development of the visual system. *Hum Brain Mapp 32:935–946, 2011.*   © 2010 Wiley-Liss, Inc.

Key words: diffusion; DTI; tractography; children, development; visual; dorsal; ventral

---

INTRODUCTION

Visual perception shows a rapid rate of maturation during the first years of life. However, visual perceptual functions seem to differ in the speed of development and some visual perceptual skills may not be mature until adolescence [Atkinson, 2000]. Recent studies have attempted to investigate the underlying mechanisms of visual development by looking at the course of development of functionally specialized brain areas. Mature visual systems were found to be segregated into two functionally specialized pathways, the occipitoparietal or "dorsal" stream and the occipitotemporal or "ventral" stream [Haxby et al., 1991; Hubel and Livingstone, 1987; Ungerleider and Mishkin, 1982]. Dorsal stream functions are associated with spatial processing and the control of visually guided actions, while ventral stream functions are committed to perceptual identification [Goodale and Milner, 1992]. It has been shown that children at the age of 7 years are able to identify objects or biological stimuli such as humans or animals even on the basis of scarce visual information [Pavlova et al., 2001]. High-order perceptual functions, however, such as detection of biological stimuli based on point-light motion within noise, visual-spatial integration, or detection of objects under uncommon viewpoints, may not mature until late adolescence or early adulthood [Freire et al., 2006; Jüttner et al., 2006; Kovács et al., 1999; Rentschler et al., 2004].

The anatomical foundations underlying visual development remain unclear. Some studies on visual development suggested that one of the streams may mature later than the other without providing neuroimaging evidence for this effect [Jüttner et al., 2006; Kovács et al., 1999; Rentschler et al., 2004]. In a few cases, functional brain imaging studies have demonstrated that dorsal stream areas develop late [Klaver et al., 2008; Lichtensteiger et al., 2008], but specialized areas related to perceptual identification and memory of faces and objects within the ventral stream have also been shown to be immature at age 7 [Gathers et al., 2004; Golarai et al., 2007]. One important way to investigate large scale functional networks is by searching for the white matter connections underlying these networks [Gong et al., 2009]. To our knowledge, no previous studies have compared the development of the dorsal and ventral streams directly, or looked at the development of the connectivity between these streams.

Since DTI enables the detection and evaluation of white-matter microstructure, it is a valuable tool for investigating typical and atypical changes during white matter maturation [Barnea-Goraly et al., 2005; Ben Bashat et al., 2005; Hüppi et al., 2001; Lebel et al., 2008; Mukherjee et al., 2001; Paus et al., 1999]. Previous studies have revealed age-related increases in fiber tract volumes within several major trajectories, including those within the visual system. Since there is evidence that the fiber density does not increase after birth the aggrandising fiber volume is thought to originate from the ongoing axonal myelination, resulting in an overall increase of fiber diameters [Jito et al., 2008; LaMantia and Rakic, 1990; Paus et al., 2001]. Along with the protracted structural arrangement of fibers into tight bundles and increasing white matter volumes those maturational processes strongly modulate observable changes in DTI measurements, resulting in increasing fractional anisotropy (FA) and axial diffusivity (AD) along with reduced radial diffusivity (RD) and mean diffusivity (MD) [Hasan et al., 2009; Lebel et al., 2008; Morriss et al., 1999; Suzuki et al., 2003].

To date, just a few DTI studies have focused on the development of the visual system and related white matter maturation for high order visual functions such as visual working memory or visual search. These studies have shown that trajectories mature late in a broad network, including connections between parietal and frontal regions [Klingberg, 2006; Mabbott et al., 2006]. Studies on the microstructural development of the corpus callosum (CC) have suggested that abundant reorganization takes place in the splenium of the CC [Innocenti et al., 1995]. The splenium is comprised of myelinated fibers that connect occipital, parietal, and temporal brain regions and may play an important role in visual development during childhood and adolescence [Hasan et al., 2009]. In addition, FA was recently found to increase in most major tracts in the brain from age 5 to age 30 years [Lebel et al., 2008]. The authors defined mature fiber tracts as those demonstrating 90% of its maturational plateau in FA. They reported that association fibers in the inferior longitudinal fascicle (ILF) finished maturation earlier than commissural fibers, while projection fibers were found to mature latest. Their results opposed those of earlier studies who suggested a different sequence of development based on WM maturation in term born or preterm born infants [Partridge et al., 2004; Shimony et al., 1999]. A second important suggestion was that the FA increase was highest in the thalamus and in cortical WM. The authors suggested that the FA increase in major tracts might finish earlier than the FA increase in the start and end points of trajectories, due to late rearrangement of white matter connections bordering on gray matter structures.

To capture visual stream fiber connections in this study, we assumed that fiber connections pass through white matter structures adjacent to occipital and parietal gray matter (dorsal stream), and between occipital and temporal gray matter (ventral stream) [Haxby et al., 1991; Ungerleider and Mishkin, 1982]. The ventral stream may be supported by U-curved fibers connecting nearby cortico-cortical regions within the temporal lobe, and the ILF [Conturo et al., 1999]. By contrast, the dorsal stream does not appear to be supported by major white matter connections between occipital and parietal white matter but may be supported by either U-curved fibers or long range fibers that have the visual system as trajectory destination [Mori et al., 2005]. Gong et al. reported that bilateral precuneus and middle occipital gyrus are important hubs connecting cortical structures. The connections between

parietal and occipital cortex were suggested to contain inter- and intrahemispheric fiber trajectories, but they did not explicitly report the specific anatomical structures contributing to these connections [Gong et al., 2009]. For our purpose, we did not want to restrict our search for dorsal and ventral visual pathways to predefined white matter fiber structures. Hence, we chose to segment dorsal and ventral streams based on cortical, rather than on white matter structures. Next, we identified adjacent white matter structures by region growing and performed a two ROI approach for fiber tracking between seeds and targets (and the reverse for validation) within each visual stream and in each hemisphere separately [Mori and van Zijl, 2002]. Finally, we segmented the principal white matter structures to identify those white matter structures overlapping with the dorsal and ventral streams [Conturo et al., 1999; Mori et al., 2005; Wakana et al., 2004]. Brodmann area 7 (BA7) was chosen as a target cortical structure for the dorsal stream since BA7 is cytoarchitecturally regarded as an undifferentiated precursor zone for all parietal areas and is functionally associated with dorsal visual processing [Haxby et al., 1991; Milner and Goodale, 1995; Orban et al., 2006; Waberski et al., 2008]. Brodmann area 37 (BA37) is anatomically adequately located and has the appropriate functional properties to be regarded as a ventral stream area [Grill-Spector et al., 2008; Haxby et al., 1991; Milner and Goodale, 1995]. Although the primary visual cortex would be an ideal starting point for the dorsal and ventral streams, our fiber tracking algorithm did not resolve connections between closely connected regions (BA17, 18, and 19) within the occipital cortex. To avoid losing connections, we combined these areas in a single region. Children (age 5–7 years) and adults (age 20–32 years) were compared with each other to identify quantitative DTI properties of each visual stream and to investigate qualitative differences in microstructural architecture of dorsal and ventral streams. We hypothesized an increase of fiber tract volumes and maturational differences of the fiber architecture of both visual streams. On the basis of findings that parietal WM structures mature late and temporal WM structures such as the inferior longitudinal fasciculus mature early, we expected both effects to be more pronounced within the dorsal stream [Klingberg, 2006; Lebel et al., 2008]. We further hypothesized developmental changes in the main DTI indices, i.e. age-related decreases in MD and RD and increases in FA and AD, with different microstructural and developmental characteristics between the two visual pathways.

METHODS

Participants

Twelve normally achieving children (mean age: 6.6 yrs, range: 5.4–7.8 yrs, 4 females) and 12 adults (mean age: 27.9 yrs, range: 20.2–32.9 yrs, 6 females) participated in the study after recruitment from local primary schools and the local community. All participants were right-handed as assessed by the Edinburgh Handedness Inventory. Data from one child were excluded, due to extensive head motion during the scan. To improve compliance, alleviate anxiety, and to reduce head motion, children were first introduced to the scanning procedure by a cartoon. Next, a teddy bear was positioned on the scanner table to explain and simulate the scanning procedure. They could view a short movie via video-goggles during scanning and were given a book voucher in appreciation for their participation. Adult participants received financial compensation. The study was approved by the ethics committee of the University and the State of Zurich. All adult subjects and the legal guardians of the children gave written informed consent consistent with the Declaration of Helsinki.

Data Acquisition and Analysis

DTI was performed on a 3.0T whole-body MR system using a standard eight-channel array head coil. Images were sampled along 21 different encoding directions by repeating with a diffusion-weighted single-shot double-spin-echo sequence. An effective b-value of 1,000 s/mm^2 was used for each of the 21 directions. To allow post hoc motion correction, five additional b0 measurements with a b-value of 0s/mm^2 were interleaved with the diffusion encoding scans. The DTI scan parameters were: repetition time (TR): 12.5 s, echo time (TE): 99.2 ms, image matrix size: 128 × 128, and FOV: 220 × 220 mm^2. Thirty-nine contiguous 3-mm thick axial images were acquired parallel to the anteroposterior commissural line. All participants additionally volunteered for a functional MRI study. These fMRI data are published elsewhere [Lichtensteiger et al., 2008].

DTI data processing and fiber tracking was performed in the native space of each subject. The five interleaved b0 volumes were motion corrected using an affine algorithm. Resulting transformation matrices were stepwise applied to the subsequent diffusion encoded image volumes (Diffusion Toolbox, sourceforge.net/projects/spmtools, SPM5, www.fil.ion.ucl.ac.uk/spm). Diffusion tensors, FA, MD, AD, and RD maps were calculated using the same software. Tensor data and maps of the diffusion indices were then transformed into a data format amenable to the DTI&Fiber Tools software package for fiber tracking and visualization [Kreher et al., 2005] using an in-house Matlab^{TM} interface. A deterministic fiber tracking algorithm [Mori et al., 1999] was applied to the whole brain by placing one fiber seed at the centre of each voxel of the data volume. To identify the main cerebral fiber skeleton, the following stop criteria were applied: FA value drops below 0.2 or MD exceeds 0.002. Fibers were also terminated if the angle between the principal eigenvectors of adjacent voxels exceeded 53.1° [Kreher et al., 2005].

Cerebral brain and fiber volumes were estimated to control for global anatomical differences between age groups. Cerebral brain volumes were estimated by masking the individual DTI brain volumes with the standard Montreal Neurological Institute (MNI) brain mask. This procedure involved transformation of the MNI brain mask into native subject space, skull stripping the volumes, removal of the cerebellum by using a mask that was defined in WFU Pickatlas v.2.4 [Maldjian et al., 2003], segmenting the volumes into gray matter, white matter and cerebrospinal fluid, and counting the total number of voxels of the resulting gray matter. Cerebral fiber volumes were derived from the individual FA volumes by applying the criteria used for fiber tracking (FA > 0.2; MD < 0.002). Cerebral brain and fiber volumes were tested for group differences by means of independent samples t-test statistics. Reported volumes were not corrected for brain volumes, since total brain volume did not show significant differences between groups. Testing the volumes by applying corrected values did not change the results.

To analyse properties of visual system fiber trajectories, a set of anatomical gray matter regions-of-interest (ROI) were generated, depicting early visual processing areas (BA17, BA18, and BA19) as well as dorsal (BA7) and ventral (BA37) visual areas, for each hemisphere separately using WFU Pickatlas. ROIs were transferred into native subject space using inverted deformation fields based on the transformation matrices from MNI space normalization of the individual mean b0 images (SPM5 Deformations utility). Next, ROIs underwent region growing only within white matter until a white matter ROI volume of 1 cm^3 was reached. Individual ROI volumes were transformed into DTI&Fiber Tools data format and used as seed and target regions in a two-ROI-approach to select corresponding fibers [Mori and van Zijl, 2002]. Trajectories of the left dorsal stream were determined between white matter ROIs adjacent to left parietal (BA7) and occipital (BA17, BA18, and BA19) ROIs. Similarly, the right dorsal stream was determined for the right hemisphere ROIs. Trajectories of the ventral streams were determined between white matter ROIs adjacent to temporal (BA37) and occipital (BA17, BA18, and BA19) ROIs within each hemisphere. White matter ROIs served as seeds and targets in the two-ROI approach to verify the algorithm. There was no significant difference either way the algorithm was applied. Binary visit-masks of all fiber tracts were estimated and transferred from each subject's native space into common MNI space by applying the transformation matrix obtained from nonlinear normalization of the mean b0 images. These visit-masks, representing all voxels intersecting with fibers of a specific tract, were used to extract fiber tract volume (number of voxels) and specific DTI indices (FA, MD, AD, and RD). We applied Gaussian fitting to test for the distribution of indices across voxels within each individual visit-mask and found median values to best represent the data. DTI indices were statistically analyzed within SPSS v.14.0 applying repeated measures ANOVA with within-subjects variables path (dorsal, ventral) and hemisphere (right, left), and between-subjects factor group (children, adults). Post hoc t-test analysis was used to further specify developmental differences. Applying a Bonferroni correction for multiple comparisons to obtain an alpha level of 0.05 resulted in a statistical threshold for significance of $P < 0.00625$.

To characterize maturation of visual system WM architecture, the following steps were undertaken. First, visitmasks were group-wise averaged to obtain fiber tract probability maps for the left and right dorsal and ventral visual streams. Second, a threshold of 60% within-group concordance was applied. Third, the resulting binary group visit-masks were segmented into fiber structure compartments. In accordance with previous work describing visual temporal lobe connections [Catani et al., 2003], the following fiber structures were tracked to parcel the individual ventral and dorsal streams into tract compartments: posterior corpus callosum (PCC), posterior thalamic radiation (PTR), inferior longitudinal fascicle (ILF), inferior fronto-occipital fascicle (IFO), and superior longitudinal fascicle (SLF) [Conturo et al., 1999; Mori et al., 2002]. Uncinate fasciculus, posterior region of the corona radiate, and anterior thalamic radiation were also tracked, but not reported here since no tracts of the dorsal or ventral visual streams were found to overlap with these structures. Finally, to test developmental differences in the fiber composition and connectivity of the dorsal and ventral visual pathways, the contribution of each aforementioned anatomical tract compartment and the overlap between anatomical tract compartments were logically compared between age groups. This analysis is thought to provide a descriptive estimation of anatomical differences in fiber tractography between adults and children.

RESULTS

Tract Volumes

Table I shows volume properties of the whole brain (gray and white matter), total white matter, and dorsal and ventral visual stream fiber tracts. Cerebral volumes showed no significant group difference and visual stream fiber tract volumes also revealed no significant difference between children and adults. Repeated measures ANOVA on visual stream fiber tract volumes yielded a significant difference in path ($F_{1,21} = 19.77$, $P < 0.001$) and in the interaction between path and group ($F_{1,21} = 10.67$, $P < 0.005$). Dorsal stream fiber tract volumes were larger in adults than in children, while ventral stream tract volumes did not differ between groups (dorsal: $t_{21} = -3.41$, $P < 0.005$; ventral: $t_{21} = -0.53$, $P > 0.5$). Paired t-test analysis on path revealed significantly larger dorsal than ventral stream fiber tract volumes for adults only (adults: $t_{11} = 5.71$, $P < 0.001$; children: $t_{10} = 0.80$, $P > 0.1$). No significant volume differences between hemispheres or interactions with group were found.

TABLE I. Mean cerebral volumes, white matter volumes, and fiber tract volumes of children and adults

	Group	Mean volume [voxel]	SD (volume) [voxel]	t	Sig. (2-tailed)
Total cerebral volume	children	122,269.36	18,255.197	−0.242	$P = 0.811$
	adults	124,036.42	16,820.065		
Total white matter volume	children	62,819.36	10,707.647	−0.775	$P = 0.447$
	adults	66,017.83	9,075.95		
dorsal stream fiber tract volume	children	764.36	456.064	−3.407	$P = 0.003*$
	adults	1,295.17	277.377		
ventral stream fiber tract volume	children	677.46	265.924	−0.527	$P = 0.604$
	adults	728.33	194.644		

Group differences were estimated by means of independent sample t-test (children vs. adults) statistics. One voxel corresponds to 8.875 mm^3.

*$P < 0.00625$ is regarded to be significant after Bonferroni's correction for multiple comparisons.

DTI Indices

Figure 1A–D shows FA, MD, AD, and RD for each age group, visual stream, and hemisphere.

Fractional anisotropy

Mean FA of the visual streams seems to be higher for adults than for children and age-related differences seem more pronounced within the dorsal streams than the ventral streams. These observations were confirmed by repeated measures ANOVA, which exhibited a significant main effect for the between-subject factor group ($F_{1.21} = 14.03$, $P = 0.001$) and interaction between path and group ($F_{1.21} = 5.50$, $P < 0.029$). Additionally, the within-subject factors path ($F_{1.21} = 40.34$, $P < 0.001$) and hemisphere were significant ($F_{1.21} = 11.54$, $P = 0.003$), indicating higher FA values for dorsal than ventral stream fiber tracts and higher FA values for right than left hemisphere tracts.

Mean diffusivity

Higher MD indices were found for children than adults (group: $F_{1.21} = 18.20$, $P < 0.001$) and for ventral stream more than for dorsal stream (path: $F_{1.21} = 39.69$, $P < 0.001$). A significant interaction path by hemisphere ($F_{1.21} = 32.47$, $P < 0.001$) indicated higher ventral than dorsal stream indices in the left hemisphere.

Axial diffusivity

Mean AD for adults and children seemed to differ between pathways as confirmed by a significant interaction between path and group ($F_{1.21} = 10.00$, $P = 0.005$). This may be due to a larger difference between AD values of adult dorsal and ventral stream, or because ventral stream AD values tended to be lower for adults than for children. Furthermore, the right dorsal stream yielded large AD values as revealed by a significant interaction between path and hemisphere ($F_{1.21} = 33.13$, $P < 0.001$). Main effects of path ($F_{1.21} = 141.42$, $P < 0.001$) and hemisphere ($F_{1.21} = 14.06$, $P = 0.001$) were also significant.

Radial diffusivity

Mean RD was higher for children than adults (group: $F_{1.21} = 22.03$, $P < 0.001$) and for ventral stream more than for dorsal stream (path: $F_{1.21} = 72.22$, $P < 0.001$). A significant interaction was found between path and group ($F_{1.21} = 5.34$, $P = 0.031$), indicating that RD differences between age groups were larger in the dorsal than ventral stream. The main effect of hemisphere ($F_{1.21} = 9.06$, $P = 0.007$) and interaction between path and hemisphere ($F_{1.21} = 5.76$, $P = 0.026$) were also significant.

Fiber Architecture

Figure 2 shows visual stream fiber tract structures in each hemisphere that are common to all subjects or exclusively present in adults or children. Tables II and III show statistics of the number of voxels that overlap between anatomical and visual stream fiber tract structures, and between anatomical fiber tract structures within each visual stream fiber tract structure, respectively.

Left dorsal stream

Common fiber tracts for adults and children were found in WM structures adjacent to the left cuneus, left middle occipital gyrus (MOG), left middle temporal gyrus (MTG), bilateral precuneus, and inferior parietal lobule. Partial overlap was found with WM structures of the PCC and left PTR. Fibers of the left PTR and PCC partly overlapped. Adults showed additional fiber structures adjacent to the left cuneus, right BA19, bilateral posterior cingulate gyrus, MTG, BA18, and BA7. These fibers reflected mainly enlarged core fiber skeletons in the PCC and bilateral PTR.
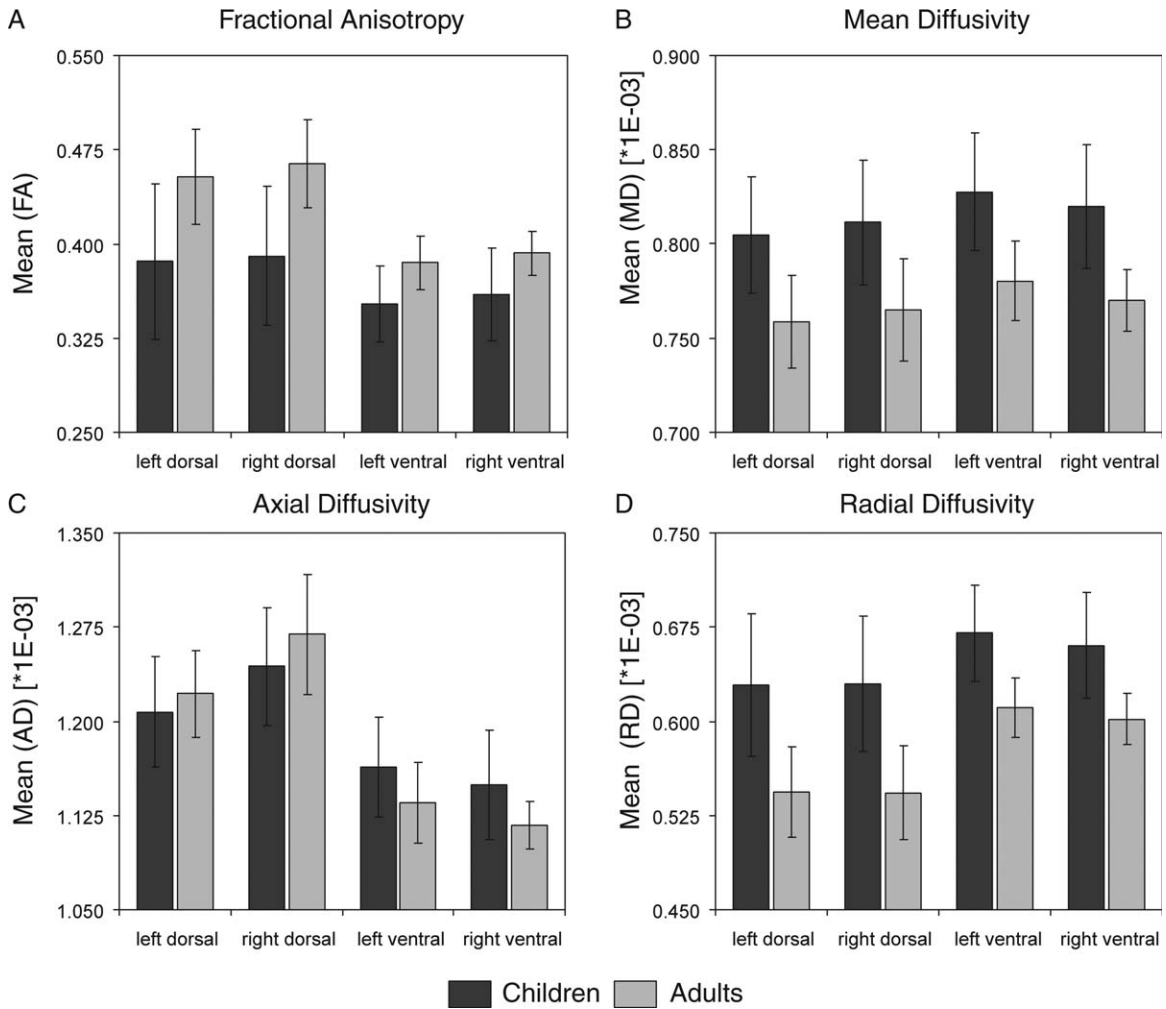
Figure 1.
Bar graphs of (**A**) mean FA, (**B**) mean MD, (**C**) mean AD, and (**D**) mean RD for the left dorsal, right dorsal, left ventral, and right ventral visual streams of children (dark gray) and adults (light gray). Presented values represent mean group indices derived from the union of the adult and children group visit-masks after applying a threshold of 60% within-group concordance. Error bars symbolize standard deviations.

Fibers of the PCC were found to partially overlap with bilateral PTR. Children showed additional fibers adjacent to the left MOG, BA7, cuneus, and precuneus. These structures overlapped with the PCC, left PTR, ILF, and SLF, but about 50% of these fibers could not be unambiguously identified.

Right dorsal stream

Common fiber tracts in adults and children include WM structures adjacent to right cuneus, precuneus, MOG, and MTG, bordering right extrastriate visual areas (BA18 and BA19), dorsal posterior cingulate (BA31), and superior parietal lobule (BA7). These fiber tracts were mostly comprised of the PCC but also included smaller portions of the right ILF and bilateral PTR. A partial overlap was found between fiber structures of the PCC and right PTR, PCC and right ILF, right PTR and ILF. Adults revealed fiber tracts adjacent to the contralateral agranular retrolimbic cortex (BA30), right primary visual cortex (BA17), and superior temporal gyrus. The increase in volume accompanied an overlap with PCC, bilateral PTR, ILF, and IFO. The PCC showed an overlap with bilateral PTR, but more importantly, dorsal tracts penetrated into temporal lobe regions by showing overlap of the PCC and PTR with bilateral IFO and ILF. Children revealed only additional fiber structures overlapping with the PCC.
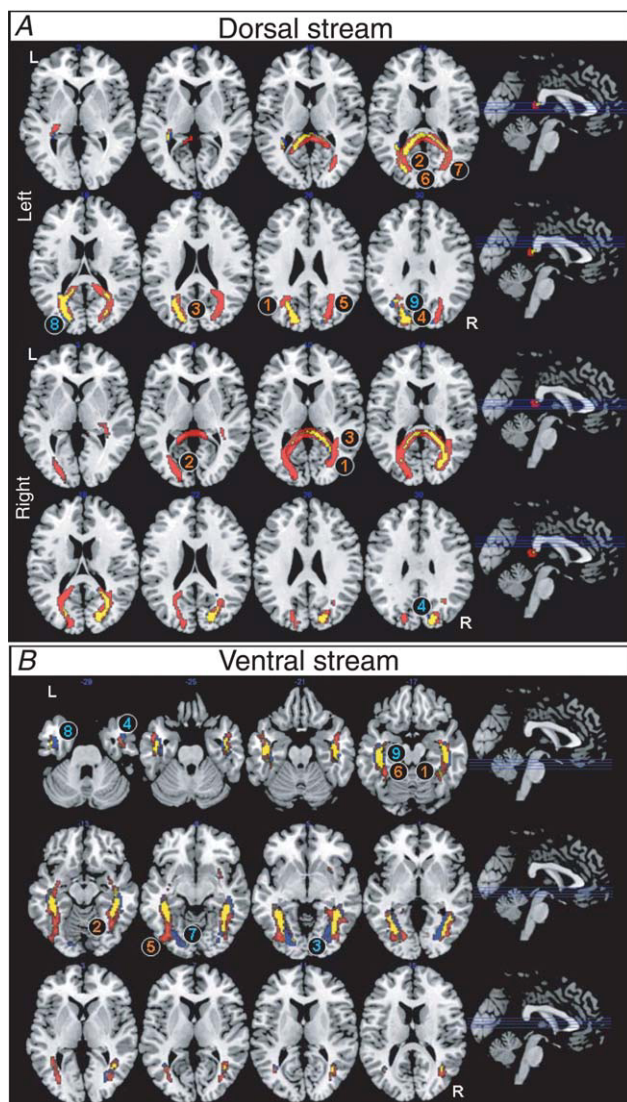
Figure 2.

Dorsal (**A**) and ventral streams (**B**) (neurological convention, axial view) representing voxels with 60% or more within group concordance. Common fiber tracts of both groups are marked in yellow; fibers exclusively found in adults are red and those exclusively found in children blue. Labels refer to areas of major differences in the fiber architecture of adults (red) and children (blue) as described in the text. Dorsal streams are separately displayed for left (top) and right (bottom) streams. As left and right ventral stream structures do not overlap they are combined in one figure. 2A-top: (1) left middle temporal gyrus (MTG), (2) left cuneus, (3) bilateral posterior cingulate gyrus (PCG), (4) bilateral inferior parietal lobule (IPL), (5) right MTG, (6) bilateral BA18, (7) right BA19, (8) left middle occipital gyrus (MOG), (9) left BA7, cuneus, and precuneus; 2A-bottom: (1) right BA17, (2) left BA30, (3) right STG, (4) right BA19. 2B: (1) right BA36, (2) right BA37, (3) right lingual gyrus, (4) right BA21, (5) left IOG, (6) left BA36, (7) left BA18, (8) left BA20, (9) left BA36. [Color figure can be viewed in the online issue, which is available at wileyonlinelibrary.com.]

Left ventral stream

Fiber tracts common in adults and children were located adjacent to left inferior temporal gyrus (ITG), MOG, parahippocampal gyrus (PHG), and fusiform gyrus (FG). They bordered BA19, BA20, BA36, and BA37. The tracts partly overlapped with left ILF, IFO, and PTR. Note that ILF and IFO are contiguous in a great part of their trajectory resulting in large overlap of volumes. A small tract part overlapped with the SLF. Adults revealed exclusive fibers next to left inferior occipital gyrus (IOG) and BA36 that overlapped with IFO, ILF, and PTR. Children yielded additional bundles adjacent to left lingual gyrus (BA18), ITG (BA20), and PHG (BA36) that also overlapped with IFO, ILF, and PTR.

Right ventral stream

Fiber tracts common to both groups encompassed right hemisphere WM structures next to MTG, IOG, PHG, and FG, that bordered on BA7, BA18, BA19, and BA31. The structure included parts of right ILF, IFO, and PTR. Adults exclusively revealed mainly tracts next to right BA36 and BA37 that overlapped with ILF, IFO, and PTR, while children yielded exclusive fiber bundles adjacent to the right lingual gyrus and BA21 that also overlapped with ILF, IFO, and PTR.

DISCUSSION

The aim of this study was to investigate the microstructural development of dorsal and ventral visual streams. In line with our hypothesis, we found evidence for age differences in volume and DTI parameters particularly in the dorsal stream. A novel finding was that maturation is reflected in the fiber connectivity of both visual pathways. The dorsal stream fiber architecture showed age differences in terms of greater inter-hemispheric connectivity and augmenting connections between dorsal and ventral streams. The ventral visual stream of children was almost adult-like, although the trajectories within the ventral stream suggested reorganization between children and adults of the fiber pathways from medial to lateral temporal cortex.

White Matter Indices of the Visual System

Age-dependent white matter indices support and extend previous results on fiber development [Giedd et al., 1999; Hasan et al., 2009; Lebel et al., 2008; Paus et al., 2001]. Core fiber skeletons increased in volume by a factor 2 to 3 for PCC fiber bundles and by 1.5 to 2 for PTR fibers within the dorsal stream. Ventral stream structures did not change in volume. Volume changes were more prominent within the right dorsal streams and may partly reflect protracted fiber myelination of commissural and projection trajectories. Fiber diameters are known to range from

TABLE II. Composition of dorsal and ventral visual fiber streams [posterior corpus callosum (PCC), posterior thalamic radiation (PTR), inferior longitudinal fasciculus (ILF), inferior fronto-occipital fasciculus (IFO), and superior longitudinal fasciculus (SLF)]

Path	Hemisphere	Group	Total	Not identified	Right SLF	Left SLF	Right PTR	Left PTR	Right ILF	Left ILF	Right IFO	Left IFO	Bilateral PCC
Dorsal	Right	Common (children and adults)	569	—	—	—	59	1	18	—	—	—	519
		Exclusively adults	1,302	—	—	—	150	113	46	40	21	2	1,210
		Exclusively children	60	36	—	—	—	—	—	—	—	—	24
	Left	Common (children and adults)	698	—	—	—	1	110	—	6	—	—	586
		Exclusively adults	938	135	—	—	59	22	1	6	-	-	715
		Exclusively children	193	91	—	3	—	66	—	13	—	—	20
Ventral	Right	Common (children and adults)	734	—	—	—	16	—	633	—	336	—	1
		Exclusively adults	240	87	—	—	19	—	104	—	30	—	—
		Exclusively children	253	—	—	—	14	—	214	—	96	—	—
	Left	Common (children and adults)	574	—	—	4	—	26	—	553	—	313	—
		Exclusively adults	268	—	—	4	—	31	—	185	—	95	6
		Exclusively children	441	—	—	2	—	33	—	358	—	158	—

Values represent volumes (in voxels, 1 voxel $==$ 8.875 mm^3) of contributing anatomical fiber structures.

about 0.1 μm for nonmyelinated to 0.4–5.0 μm for myelinated axons [Aboitiz et al., 1992], which could well account for the volume changes. We further observed an age-related increase in FA and a decrease in MD and RD within both visual streams. FA increase and RD decrease were particularly strong in the dorsal stream. These findings extend earlier findings about development of major trajectories. Most important trajectories that were found to be part of dorsal (PCC and PTR) and ventral streams (IFO and ILF) increase in FA and decrease in MD between 5 and 30 years [Lebel et al., 2008]. Lebel et al. showed that the FA in the ILF increased most rapidly between 5 and 7 years, and remained stable after age seven. It therefore seems plausible that FA does not increase much in ILF in our group, since the average age was 6 years. Hence, the early maturation of the ILF may account for the small difference in FA within the ventral visual stream between age groups in our study. The reduction in RD fits with the hypothesis that unrestricted myelination decreases unrestricted extra-axonal water, resulting in a higher decrease in RD compared with AD [Suzuki et al., 2003]. The finding that AD tended to decrease in the ventral stream and increase in the dorsal stream may reflect differences in the gradation of axonal flow [Suzuki et al., 2003] or fiber compactness [Van Essen, 1997] that accompanies maturation.

Age-related hemispheric differences were not found for the DTI indices. However, children and adults both revealed lateralization effects for MD and AD between the dorsal streams. Independent of age both diffusivities were higher within the right hemisphere. To our knowledge no previous study on comparable WM structures reported hemispheric differences in any of the DTI indices [Bonekamp et al., 2007; Snook et al., 2005]. One possible explanation is that the observed pattern of changes in MD and AD reflect hemispheric differences in fiber packing [Van Essen, 1997]. However, we consider this unlikely. Rather, we suggest that the overlap of the right dorsal stream with few main WM structures may account for the high alignment and structural organization of the dorsal stream. By contrast, the high number of adjacent and crossing trajectories in the ventral stream and close alignment to cortical structures may reduce AD. Nevertheless, further studies are warranted to explain these effects.

Connectivity Within the Visual System

Generally, the ventral stream followed the expected overlap with the ILF and IFO along the temporal lobe. In contrast, the dorsal stream did not follow the direct way between the occipital and parietal lobes, as would have been expected on the basis of functional imaging data [Haxby et al., 1991; Orban et al., 2006]. Rather, we found fibers that penetrated through white matter structures in occipital and parietal lobes and run along the main structures of the PCC and PTR. As can be seen in Figure 2, these dorsal stream fibers share the thalamic respectively contralateral destinations of these tracts. This is in line with previous results from adult DTI data and postmortem anatomy showing PTR and PCC fibers that partially cross borders between occipital and parietal white matter structures [Mori et al., 2002]. Our data also support and extend results reported by Gong et al. They showed that precuneus and middle occipital cortex serve as important "hubs" for connecting networks of cortical structures within and beyond the visual system. These hubs take advantage of both inter and intracortical fiber trajectories [Gong et al., 2009]. On the basis of our data, one might hypothesize that age related differences in the dorsal stream also affect connectivity between these hubs.

TABLE III. Dorsal and ventral visual stream volumes (in voxels, 1 == 8.875 mm³) containing overlapping fiber fractions of posterior corpus callosum (PCC), posterior thalamic radiation (PTR), inferior longitudinal fasciculus (ILF), inferior fronto-occipital fasciculus (IFO), and superior longitudinal fasciculus (SLF)

	Pathway											
	Left dorsal			Right dorsal			Left ventral			Right ventral		
Cohort shared by	Common	Only adults	Only children	Common	Only adults	Only children	Common	Exclusively adults	Exclusively children	Common	Exclusively adults	Exclusively children
Left SLF and left PTR	—	—	3	—	—	—	—	4	—	—	—	—
Left SLF and left ILF	—	—	1	—	—	—	4	4	2	—	—	—
Left SLF and left IFO	—	—	—	—	—	—	4	3	—	—	—	—
Left PTR and left ILF	6	6	13	—	32	—	26	31	33	—	—	—
Left PTR and left IFO	—	—	—	1	2	—	26	31	29	—	—	—
Left PTR and PCC	86	16	2	—	113	—	—	6	—	—	—	—
Left ILF and left IFO	—	—	—	—	2	—	313	95	157	—	—	—
Left ILF and PCC	4	6	—	—	40	—	—	6	—	—	—	—
Left IFO and PCC	—	—	—	—	2	—	—	6	—	—	—	—
Right PTR and right ILF	—	1	—	17	46	—	—	—	—	15	12	12
Right PTR and right IFO	—	—	—	—	21	—	—	—	—	11	9	10
Right PTR and PCC	1	59	—	59	101	—	—	—	—	1	—	—
Right ILF and right IFO	—	—	—	—	21	—	—	—	—	336	30	96
Right ILF and PCC	—	1	—	18	30	—	—	—	—	1	—	—
Right IFO and PCC	—	—	—	—	14	—	—	—	—	1	—	—

Developmental changes of fiber architecture were found within both visual pathways. The dorsal stream undergoes major architectural changes between age 6 and adulthood. We observed a larger number of inter-hemispheric fiber connections in both left and right dorsal streams. Here, the tracking algorithm found more fibers in adults than in children across callosal fibers into structures that overlapped with ipsilateral association and projection fibers in the ipsilateral and contralateral hemisphere. This pattern was particularly prominent within the right hemisphere dorsal visual stream where more fibers were found in adults than in children in bilateral parietal, temporal, and occipital structures. One possibility is that fibers are connected to each other through axonal synapses [Innocenti et al., 1995]. Alternatively, pruning may facilitate finding fiber solutions as reduction of fiber crossing and kissing decreases ambiguity in microstructural organization within voxels [Mori and van Zijl, 2002]. In any case, the observation that interhemisphere connectivity is higher in adults than in children is consistent with studies on development of the CC [Hasan et al., 2009]. The finding that adults showed additional fibers in ipsilateral structures of the IFO and ILF is new and suggests that intrahemispheric connectivity increases between childhood and adulthood, but the functional relevance of this finding needs to be investigated further. One hypothesis is that higher cognitive functions, including the development of dorsal stream function, require organized inter and intrahemisphere connectivity [Aboitiz and Montiel, 2003; Baizer et al., 1991]. The development of these functional networks may not be mature at age 6 [Freire et al., 2006; Klaver et al., 2008; Kovács et al., 1999; Lichtensteiger et al., 2008].

The core fiber skeletons of ventral stream tracts did not differ between the two age groups. However, the spatial organization of fiber tracts neighboring right-hemisphere temporal cortical structures showed high variations between groups. Adult subjects showed additional fiber bundles adjacent to the right temporo-occipital junction, i.e., to areas that are specialized for processing different visual semantic categories [Grill-Spector, 2003]. This result is in line with behavioral and neuroimaging studies on the development of processing visual semantic categories [Gathers et al., 2004; Golarai et al., 2007; Klaver et al., 2008; Lichtensteiger et al., 2008]. Adults also showed more fiber tracts adjacent to the left inferior occipital gyrus, while the children's ventral stream tracts extended further toward the left lingual areas BA18 and BA19. Although the functionality of the architectural reorganization cannot be verified in this study, the additional trajectories between adult left lateral temporal cortex and anterior temporal cortex may support functional connectivity between areas specialized for processing visual word forms and language [Mechelli et al., 2005; Price, 2000; van der Mark et al., 2009].

There are some limitations to this study. (1) We applied a deterministic fiber tracking approach, which, although widely used, has limitations for resolving crossing fibers [Mori and van Zijl, 2002]. (2) The use of a semiautomatic parcellation algorithm for the fiber structures may fail to exactly determine every tract across subjects. Individual anatomical variations may, thus, lead to either the exclusion of fibers of a particular tract or to the inclusions of fibers from other fiber structures. (3) The cross-sectional design of the study limits the detection of subtle changes due to inter-subject variation. (4) The large difference in age between groups allows no validation of subtle differences of the time-course during maturation. (5) The relatively small sample sizes of our cohorts reduce the statistical power of the study. (6) The unbalanced gender distribution of the paediatric group (7 male, 4 female) may have influence on the interpretation, particularly of the tract volumes. Schmithorst et al. [2008] recently provided evidence for significant gender differences in DTI indices of occipital, parietal, and temporal regions in children and adolescents. The limited sample size of our study did not allow for meaningful gender comparison. Hence, our results on DTI indices might be slightly detracted by the unequal gender populations. (7) Present data show high between-subject (tract volumes) and within-subject (DTI indices distribution across voxels) variability. To account for the differences in tract architecture, we allowed liberal inter-subject concordance levels of 60% for group visit-mask definition. To test for individual indices distribution across voxels, we applied Gaussian fitting and found median values to best represent the data. (8) One may argue that main differences between visual streams can be explained by the major trajectories and global developmental differences between fiber types or between inter and intrahemisphere connectivity. However, any global developmental difference between fiber types will influence the development of the visual streams, but will not limit our findings regarding the maturation of the visual system. Furthermore, analyzing and reporting developmental differences for each tract is beyond the scope of this paper and has already been reported by Lebel et al. [2008]. Also the earlier reports that association tracts mature later than other tracts are probably not valid, since ILF contains early maturing association fibers [Lebel et al., 2008]. (9) The regions of interest were chosen on the basis of functional imaging data [Haxby et al., 1991]. We have no behavioral data that support the functionality of the chosen regions. Further studies are required to resolve link between structural and functional maturation. (10) One might argue that general increase in FA might cause the tractography algorithm to identify generally larger tracts in the brain. However, this argument seems unlikely since we found different architectural differences between adults and children that cannot be explained by a general FA difference, and we found more extensive trajectories in adult right dorsal stream, although adult FA did not differ between left and right dorsal streams. (11) Finally, it is difficult to interpret differences in FA between groups in fiber structures that contain more than one major fiber tract. For example, Lebel et al. [2008] reported different age related changes in FA within the PTR and PCC, where

PTR showed a protracted development as compared with the PCC. This suggests that FA changes may be stronger within the PTR than in the PCC although these structures largely overlap. This is also in line with Hasan et al. [2009] who found age-related changes in RD but not in FA in PCC. In line with these studies, we suggest that age related FA differences in the dorsal visual stream relates to maturation of the PTR, whereas the finding that more fibers passed the PCC in adults than in children may relate to the reduced RD in the PCC.

To summarize, we found core WM fiber tract skeletons for the ventral and dorsal visual streams to be present in children with an average age of 6 years. The dorsal stream tract volumes increase significantly between childhood and adulthood and dorsal fibers extended into structures of the commissural and contralateral projection trajectories. In contrast, the volumes of the ventral pathways already reach adult-like sizes at the age of 7 years. Children exclusively presented ventral stream fiber bundles to lingual visual areas that may prune until adulthood due to experience-based plasticity. Ventral stream connections to the right fusiform and parahippocampal gyri seem to be not yet completely established in children. These findings provide additional insight into the maturational differences in visual development provided by DTI indices.

ACKNOWLEDGMENTS

REFERENCES

Aboitiz F, Montiel J (2003): One hundred million years of interhemispheric communication: The history of the corpus callosum. Braz J Med Biol Res 36:409–420.

Aboitiz F, Scheibel AB, Fisher RS, Zaidel E (1992): Fiber composition of the human corpus callosum. Brain Res 598:143–153.

Atkinson J (2000): The Developing Visual Brain. Oxford: Oxford University Press.

Baizer JS, Ungerleider LG, Desimone R (1991): Organization of visual inputs to the inferior temporal and posterior parietal cortex in macaques. J Neurosci 11:168–190.

Barnea-Goraly N, Menon V, Eckert M, Tamm L, Bammer R, Karchemskiy A, Dant CC, Reiss AL (2005): White matter development during childhood and adolescence: A cross-sectional diffusion tensor imaging study. Cereb Cortex 15:1848–1854.

Ben Bashat D, Ben Sira L, Graif M, Pianka P, Hendler T, Cohen Y, Assaf Y (2005): Normal white matter development from infancy to adulthood: Comparing diffusion tensor and high b value diffusion weighted MR images. J Magn Reson Imaging 21:503–511.

Bonekamp D, Nagae LM, Degaonkar M, Matson M, Abdalla WM, Barker PB, Mori S, Horska A (2007): Diffusion tensor imaging in children and adolescents: reproducibility, hemispheric, and age-related differences. Neuroimage 34: 733–742.

Catani M, Jones DK, Donato R, Ffytche DH (2003): Occipitotemporal connections in the human brain. Brain 126 (Part 9):2093–2107.

Conturo TE, Lori NF, Cull TS, Akbudak E, Snyder AZ, Shimony JS, McKinstry RC, Burton H, Raichle ME (1999): Tracking neuronal fiber pathways in the living human brain. Proc Natl Acad Sci USA 96:10422–10427.

Freire A, Lewis TL, Maurer D, Blake R (2006): The development of sensitivity to biological motion in noise. Perception 35:647–657.

Gathers AD, Bhatt R, Corby CR, Farley AB, Joseph JE (2004): Developmental shifts in cortical loci for face and object recognition. Neuroreport 15:1549–1553.

Giedd JN, Blumenthal J, Jeffries NO, Castellanos FX, Liu H, Zijdenbos A, Paus T, Evans AC, Rapoport JL (1999): Brain development during childhood and adolescence: A longitudinal MRI study. Nat Neurosci 2:861–863.

Golarai G, Ghahremani DG, Whitfield-Gabrieli S, Reiss A, Eberhardt JL, Gabrieli JDE, Grill-Spector K (2007): Differential development of high-level visual cortex correlates with category-specific recognition memory. Nature Neuroscience 10:512–522.

Gong G, He Y, Concha L, Lebel C, Gross DW, Evans AC, Beaulieu C (2009): Mapping anatomical connectivity patterns of human cerebral cortex using in vivo diffusion tensor imaging tractography. Cereb Cortex 19:524–536.

Goodale MA, Milner AD (1992): Separate visual pathways for perception and action. Trends Neurosci 15:20–25.

Grill-Spector K (2003): The neural basis of object perception. Curr Opin Neurobiol 13:159–166.

Grill-Spector K, Golarai G, Gabrieli J (2008): Developmental neuroimaging of the human ventral visual cortex. Trends Cogn Sci 12:152–162.

Hasan KM, Kamali A, Iftikhar A, Kramer LA, Papanicolaou AC, Fletcher JM, Ewing-Cobbs L (2009): Diffusion tensor tractography quantification of the human corpus callosum fiber pathways across the lifespan. Brain Res 1249:91–100.

Haxby JV, Grady CL, Horwitz B, Ungerleider LG, Mishkin M, Carson RE, Herscovitch P, Schapiro MB, Rapoport SI (1991): Dissociation of object and spatial visual processing pathways in human extrastriate cortex. Proc Natl Acad Sci USA 88:1621–1625.

Hubel DH, Livingstone MS (1987): Segregation of form, color, and stereopsis in primate area 18. J Neurosci 7:3378–3415.

Hüppi PS, Murphy B, Maier SE, Zientara GP, Inder TE, Barnes PD, Kikinis R, Jolesz FA, Volpe JJ (2001): Microstructural brain development after perinatal cerebral white matter injury assessed by diffusion tensor magnetic resonance imaging. Pediatrics 107:455–460.

Innocenti GM, Aggoun-Zouaoui D, Lehmann P (1995): Cellular aspects of callosal connections and their development. Neuropsychologia 33(8):961–987.

Jito J, Nakasu S, Ito R, Fukami T, Morikawa S, Inubushi T (2008): Maturational changes in diffusion anisotropy in the rat corpus callosum: Comparison with quantitative histological evaluation. J Magn Reson Imaging 28:847–854.

Jüttner M, Müller A, Rentschler I (2006): A developmental dissociation of view-dependent and view-invariant object recognition in adolescence. Behav Brain Res 175:420–424.

Klaver P, Lichtensteiger J, Bucher K, Dietrich T, Loenneker T, Martin E (2008): Dorsal stream development in motion and structure-from-motion perception. Neuroimage 39:1815–1823.

Klingberg T (2006): Development of a superior frontal-intraparietal network for visuo-spatial working memory. Neuropsychologia 44:2171–2177.

Kovács I, Kozma P, Fehér A, Benedek G (1999): Late maturation of visual spatial integration in humans. Proc Natl Acad Sci USA 96:12204–12209.

Kreher BW, Schneider JF, Mader I, Martin E, Hennig J, Il'yasov KA (2005): Multitensor approach for analysis and tracking of complex fiber configurations. Magn Reson Med 54:1216–1225.

LaMantia AS, Rakic P (1990): Axon overproduction and elimination in the corpus callosum of the developing rhesus monkey. J Neurosci 10:2156–2175.

Lebel C, Walker L, Leemans A, Phillips L, Beaulieu C (2008): Microstructural maturation of the human brain from childhood to adulthood. Neuroimage 40:1044–1055.

Lichtensteiger J, Loenneker T, Bucher K, Martin E, Klaver P (2008): Role of dorsal and ventral stream development in biological motion perception. Neuroreport 19:1763–1767.

Mabbott DJ, Noseworthy M, Bouffet E, Laughlin S, Rockel C (2006): White matter growth as a mechanism of cognitive development in children. Neuroimage 33:936–946.

Maldjian JA, Laurienti PJ, Kraft RA, Burdette JH (2003): An automated method for neuroanatomic and cytoarchitectonic atlas-based interrogation of fMRI data sets. Neuroimage 19:1233–1239.

Mechelli A, Crinion JT, Long S, Friston KJ, Lambon Ralph MA, Patterson K, McClelland JL, Price CJ (2005): Dissociating reading processes on the basis of neuronal interactions. J Cogn Neurosci 17:1753–1765.

Milner AD, Goodale MA (1995): The Visual Brain in Action. Oxford: Oxford University Press.

Mori S, van Zijl PC (2002): Fiber tracking: Principles and strategies—A technical review. NMR Biomed 15:468–480.

Mori S, Crain BJ, Chacko VP, van Zijl PC (1999): Three-dimensional tracking of axonal projections in the brain by magnetic resonance imaging. Ann Neurol 45:265–269.

Mori S, Kaufmann WE, Davatzikos C, Stieltjes B, Amodei L, Fredericksen K, Pearlson GD, Melhem ER, Solaiyappan M, Raymond GV, Moser HW, van Zijl PC. (2002): Imaging cortical association tracts in the human brain using diffusion-tensor-based axonal tracking. Magn Reson Med 47:215–223.

Mori S, Wakana S, Nagae-Poetscher LM, van Zijl PC (2005). MRI Atlas of Human White Matter. Amsterdam: Elsevier.

Morriss MC, Zimmerman RA, Bilaniuk LT, Hunter JV, Haselgrove JC (1999): Changes in brain water diffusion during childhood. Neuroradiology 41:929–934.

Mukherjee P, Miller JH, Shimony JS, Conturo TE, Lee BC, Almli CR, McKinstry RC (2001): Normal brain maturation during childhood: Developmental trends characterized with diffusion-tensor MR imaging. Radiology 221:349–358.

Orban GA, Claeys K, Nelissen K, Smans R, Sunaert S, Todd JT, Wardak C, Durand JB, Vanduffel W (2006): Mapping the parietal cortex of human and non-human primates. Neuropsychologia 44:2647–2667.

Partridge SC, Mukherjee P, Henry RG, Miller SP, Berman JI, Jin H, Lu Y, Glenn OA, Ferriero DM, Barkovich AJ, Vigneron DB (2004): Diffusion tensor imaging: serial quantitation of white matter tract maturity in premature newborns. Neuroimage 22:1302–1314.

Paus T, Zijdenbos A, Worsley K, Collins DL, Blumenthal J, Giedd JN, Rapoport JL, Evans AC (1999): Structural maturation of neural pathways in children and adolescents: In vivo study. Science 283:1908–1911.

Paus T, Collins DL, Evans AC, Leonard G, Pike B, Zijdenbos A (2001): Maturation of white matter in the human brain: A review of magnetic resonance studies. Brain Res Bull 54:255–66.

Pavlova M, Krägeloh-Mann I, Sokolov A, Birbaumer N (2001): Recognition of point-light biological motion displays by young children. Perception 30:925–933.

Price CJ (2000): The anatomy of language: Contributions from functional neuroimaging. J Anat 197:335–359.

Rentschler I, Jüttner M, Osman E, Müller A, Caelli T (2004): Development of configural 3D object recognition. Behav Brain Res 149:107–111.

Schmithorst VJ, Holland SK, Dardzinski BJ (2008): Developmental differences in white matter architecture between boys and girls. Hum Brain Mapp 29:696–710.

Shimony JS, McKinstry RC, Akbudak E, Aronovitz JA, Snyder AZ, Lori NF, Cull TS, Conturo TE (1999): Quantitative diffusion-tensor anisotropy brain MR imaging: Normative human data and anatomic analysis. Radiology 212:770–784.

Snook L, Paulson LA, Roy D, Phillips L, Beaulieu C (2005). Diffusion tensor imaging of neurodevelopment in children and young adults. Neuroimage 26: 1164–1173.

Suzuki Y, Matsuzawa H, Kwee IL, Nakada T (2003): Absolute eigenvalue diffusion tensor analysis for human brain maturation. NMR Biomed 16:257–260.

Ungerleider LG, Mishkin M (1982): Two cortical visual systems. In: Ingle DJ, Goodale MA, Mansfield RJW, editors. Analysis of Visual Behavior. Cambridge, MA: MIT Press. pp 549–586.

van der Mark S, Bucher K, Maurer U, Schulz E, Brem S, Buckelmuller J, Kronbichler M, Loenneker T, Klaver P, Martin E, Brandeis D (2009): Children with dyslexia lack multiple specializations along the visual word-form (VWF) system. Neuroimage 47:1940–1949.

Van Essen DC (1997): A tension-based theory of morphogenesis and compact wiring in the central nervous system. Nature 385:313–318.

Waberski TD, Gobbele R, Lamberty K, Buchner H, Marshall JC, Fink GR (2008): Timing of visuo-spatial information processing: Electrical source imaging related to line bisection judgements. Neuropsychologia 46:1201–1210.

Wakana S, Jiang H, Nagae-Poetscher LM, van Zijl PC, Mori S (2004): Fiber tract-based atlas of human white matter anatomy. Radiology 230:77–87.